Model Predictive Control with Fatigue-Damage Minimization through the Dissipativity Property of Hysteresis Operators

Barradas Berglind, Jesus; Wisniewski, Rafał; Jayawardhana, Bayu

Published in:
European Journal of Control

DOI:
10.1016/j.ejcon.2019.11.004

European Journal of Control 54 (2020) 140–151

Contents lists available at ScienceDirect

European Journal of Control

journal homepage: www.elsevier.com/locate/ejcon

Model predictive control with fatigue-damage minimization through the dissipativity property of hysteresis operators

Jesus Barradas-Berglind[a,b], Rafael Wisniewski[a,*], Bayu Jayawardhana[b]

[a] Automation and Control, Department of Electronic Systems, Aalborg University, Aalborg East 9220, Denmark
[b] Engineering and Technology Institute Groningen (ENTEG), University of Groningen, Groningen 9747AG, the Netherlands

ARTICLE INFO

Article history:
Received 30 January 2019
Revised 15 September 2019
Accepted 13 November 2019
Available online 21 November 2019

Recommended by Prof. T. Parisini

Keywords:
Predictive control
Hysteresis
Wind energy

ABSTRACT

In this paper, we propose an approximation method for the well-known fatigue-damage estimation of rainflow counting (RFC) using the dissipativity property of hysteresis operators that can be embedded in model predictive control (MPC) frameworks. Firstly, we revisit results that establish the equivalence between RFC to an energy dissipation property of an infinite-dimensional operator of the Preisach hysteresis model. Subsequently, we approximate the Preisach model using a finite-dimensional differential Duhem hysteresis model and propose an extended MPC scheme that takes into account the dissipated energy of Duhem hysteresis model as a damage proxy in the optimization problem formulation. Lastly, we present an example of control design for damage minimization in the shaft of a wind turbine where we illustrate the proposed strategy.

1. Introduction

For the past decade, various computational methods for predictive maintenance and fatigue-damage minimization have been studied in order to enable long-term operations of modern machines and to extend the durability of their electromechanical systems. Fatigue damage is considered as a critical factor in structures, where it is necessary to ensure a certain life span under normal operating conditions, especially in turbulent or harsh environments. These environmental conditions lead to irregular loadings, which decrease the life expectancy of structures or materials exposed to them. This is the case for wind turbines, and structures in contact with waves and uneven roads, among other examples. Fatigue is a phenomenon that occurs in a microscopic scale, manifesting itself as damage [37]. The most popular and widely used fatigue damage assessment metric is the so-called rainflow counting (RFC) method, gaining this name thanks to the analogy with rainwater running down roofs [34].

Despite its popularity and widespread usage, RFC is still a highly nonlinear numerical algorithm that includes deletions and therefore, it can only be used as a post-processing tool. As a consequence, it is always performed offline, e.g., [6] where RFC is used to benchmark different control strategies. It is thus not straightforward to incorporate RFC for real-time control where fatigue-damage variable becomes part of the control problem.

In this paper, we propose an alternative way of approximating a fatigue-damage model and of embedding it in a model predictive control (MPC) scheme. To this end, we first review the equivalence relation between fatigue-damage in the RFC sense and hysteresis operators; particularly, the variations of a Preisach hysteresis to symmetric RFC as addressed in [8]. Subsequently, we relate the variations of a certain class of Preisach hysteresis operator to its dissipated energy. Once the latter link has been established, we carry over the notion of dissipated energy as a measure of fatigue-damage to the Duhem hysteresis framework, as the Preisach models are infinite-dimensional operators. In other words, we propose a modified MPC strategy that incorporates the dissipated energy of Duhem hysteresis as a proxy to the systems' damage into the optimization problem cost function; this is illustrated in Fig. 1, where the proposed MPC strategy is portrayed and the reasoning steps to obtain the fatigue model are shown at the bottom.

Optimal control problems with Preisach hysteresis have been investigated in works such as [1]; however, it is not straightforward to include the Preisach hysteresis into the optimal control or MPC problem formulations, due to the lack of computational tractability of this infinite dimensional operator. Dissipated energy for the Preisach model has been well studied in [15,16,27]. Hence, we adopt the Duhem hysteresis framework, where the dissipated energy in the Duhem model [19,30,31] is used as a measure or proxy for accumulated damage. Note that the Duhem model can be explicitly written as a differential equation [26,41], hence

* Corresponding author at: Engineering and Technology Institute Groningen (ENTEG), University of Groningen, Groningen 9747AG, the Netherlands.
E-mail address: raf@aau.dk (R. Wisniewski).

https://doi.org/10.1016/j.ejcon.2019.11.004
0947-3580/

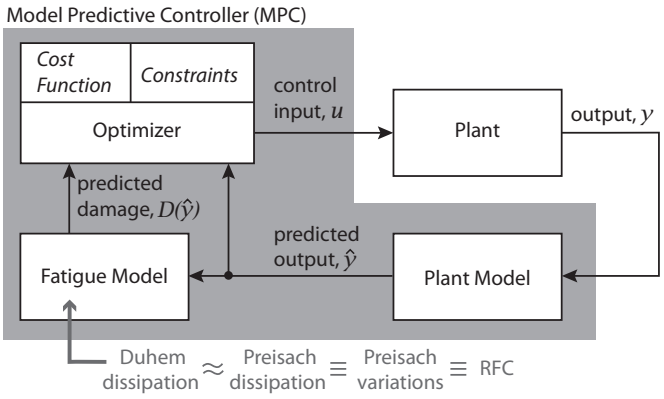

Fig. 1. Schematic showing the inclusion of fatigue model in a control loop with a model predictive controller. Note the relationships under the fatigue model, which are discussed in this paper.

facilitating its inclusion in the optimal control problem. Moreover, Duhem models have been used before to describe physical phenomena well, such as, ferromagnetics and mechanical friction [10,12]. Thus, the dissipated energy that is derived from these Duhem models can be directly interpreted as damage accumulation in the material. For instance, hysteresis loops in ferromagnetic materials induce dissipated energy as heat that translates into material changes.

The contributions of this paper are twofold: (I) the equivalence relation between Preisach hysteresis dissipated energy and damage in the RFC sense, and (II) a modified MPC strategy that includes the dissipated energy in the cost functional, where it serves as a measure of the (sub-)systems' damage. The main advantage of the proposed strategy is that control of complex physical systems with damage reduction can be numerically implemented. We demonstrate the proposed control strategy through simulations based on NREL's 5MW turbine [21]. Due to the mixed nature of the wind turbine control objectives [3,5,6], i.e., power extraction maximization and mechanical load alleviation, several optimization-based control strategies have been proposed in the literature, e.g., [36,38]. Control strategies considering wear, often called health-aware strategies, have been proposed for example for pasteurization plants [33] and water distribution networks [17]. Our proposed control method with damage reduction can be extended to different application domains, ranging from magnetics to mechanics due to the diversity of the models that can be described in the Duhem framework, such as the LuGre friction model [12], the Bouc-Wen model [18], the Coleman-Hodgdon model [10], the Dahl model [11], and the Jiles-Atherton model [20].

The remainder of the paper is organized as follows: In Section 2, we discuss the relationship between damage in the RFC sense and hysteresis operators, and in particular, we review the equivalence between the former and latter from [8]. Subsequently, in Section 3, we address the energy dissipation of the Preisach and Duhem hysteresis models; furthermore, we present an equivalent relation between dissipated energy and the variations of a particular Preisach operator, and provide an example to compare damage, total variations and dissipated energy. In Section 4, we use the dissipated energy of the Duhem model as a proxy to damage in a predictive control problem formulation, which we illustrate on a wind turbine application. Lastly, concluding remarks are given in Section 5.

2. Damage in the RFC sense and hysteresis

In this section, we discuss the relation between damage in the rainflow counting (RFC) sense and hysteresis operators. We review the equivalence between damage in the RFC sense and the variations of a Preisach hysteresis operator as proposed in [8].

The RFC method is commonly used in fatigue analysis together with the Palmgren–Miner-Rule. It is based on an algorithm that extrapolates information from extrema, i.e., maxima and minima, of a time series followed by the Palmgren–Miner rule of damage accumulation [13,40].

In Fig. 2, an example of RFC is presented together with its relation to hysteresis loops. On the left side of this figure, following the explanation in [22,34], the starting *rain* flows off all strain amplitudes as if they were roofs. The flow ends when: (i) the rain water flow meets rain water from a higher roof (e.g., E-G ends in F or C-E ends in D); (ii) the flow reaches a load value where the opposite load minimum falls below the starting minimum (e.g., 0-A-F-G with respect to H); (iii) the flow reaches a load value where the opposite load maximum is higher than the starting maximum (e.g., A-B-D-E with respect to G); (iv) there is no further roof to continue (e.g., L and T). Each rain water flow from start to end is considered as half a cycle. Half cycles of the same size, but with opposite direction result in a full cycle. Lastly, the rain flows ending in arrows at the lower part of the diagram correspond to left-over half loops. Essentially, the RFC algorithm identifies the ranges of strain which correspond to closed hysteresis loops [13]; hence, the algorithm only counts closed hysteresis loops. This is also exemplified on the right side of Fig. 2.

The previous example illustrates the relationship between the RFC algorithm and the hysteresis loops. Let us review the formal relationship between damage in the RFC sense and Preisach hysteresis operators.

For an open set $U \subset \mathbb{R}^n$, we denote $AC(U)$ as the space of absolutely continuous functions $f : U \to \mathbb{R}$. We call a continuous function $u : \mathbb{R}_+ \to \mathbb{R}$ piecewise monotone if there exists a sequence $\{t_i\}_{i\in\mathbb{N}}$ such that $t_0 = 0, t_i < t_{i+1}, \lim_n t_n \to \infty$ and the input u is monotone on each time interval $[t_i, t_{i+1}]$. The set of continuous piecewise monotone functions on $\mathbb{R}_+$ are denoted by $CPM(\mathbb{R}_+)$. For every $u \in CPM(\mathbb{R}_+)$, we define the total variation $|u|_{[0,\eta]}$ for any $\eta > 0$ by

$$|u|_{[0,\eta]} := |u(0)| + \left(\sum_{i=0}^{N-1} |u(t_{i+1}) - u(t_i)|\right) + |u(\eta) - u(t_N)|. \quad (1)$$

We define the relay operator $\mathcal{R}_{\beta,\alpha} : CPM(\mathbb{R}_+) \to CPM(\mathbb{R}_+)$, which is the basis of the Preisach operator, by

$$\big(\mathcal{R}_{\beta,\alpha}(u)\big)(t) := \begin{cases} -1 & \text{if } u(t_i) \le \beta, \\ +1 & \text{if } u(t_i) \ge \alpha, \\ -1 & \text{if } u(t) \in (\beta,\alpha) \text{ and } \big(\mathcal{R}_{\beta,\alpha}(u)\big)(t_{i-1}) = -1, \\ +1 & \text{if } u(t) \in (\beta,\alpha) \text{ and } \big(\mathcal{R}_{\beta,\alpha}(u)\big)(t_{i-1}) = +1, \end{cases} \quad (2)$$

with a given admissible initial condition $\big(\mathcal{R}_{\beta,\alpha}(u)\big)(t_0)$. Next, we define the Preisach hysteresis operator, which follows the definition given in [8] but adapted to piecewise monotone functions.

Definition 1 (Preisach hysteresis operator)**.** Let the Preisach plane be $\mathcal{P} = \{(\beta,\alpha) \in \mathbb{R}^2,\ -M \le \beta \le \alpha \le M\}$, where M is an a priori bound for admissible input values. Let the density function $\rho(\alpha, \beta)$ with compact support in $\mathcal{P}$ be given, i.e., it is zero outside $\mathcal{P}$. We define the Preisach operator $\Phi : CPM(\mathbb{R}_+) \to CPM(\mathbb{R}_+)$ by

$$\big(\Phi(u)\big)(t) := \int_{\beta<\alpha} \rho(\alpha,\beta)\big(\mathcal{R}_{\beta,\alpha}(u)\big)(t)\,d\beta\,d\alpha. \quad (3)$$

Consequently, the relevant threshold values for the relays that comprise $\Phi(u)$ will lie within the plane $\mathcal{P}$. As discussed thoroughly in [24], for all $u \in CPM(\mathbb{R}_+)$ it follows that $\Phi(u) \in CPM(\mathbb{R}_+)$.

Definition 2 (Symmetric RFC damage)**.** Let $\mathcal{N}(\alpha,\beta)$ with values β and α, chosen such that the input u with $u(t_{2i}) = \beta$ and $u(t_{2i+1}) =$

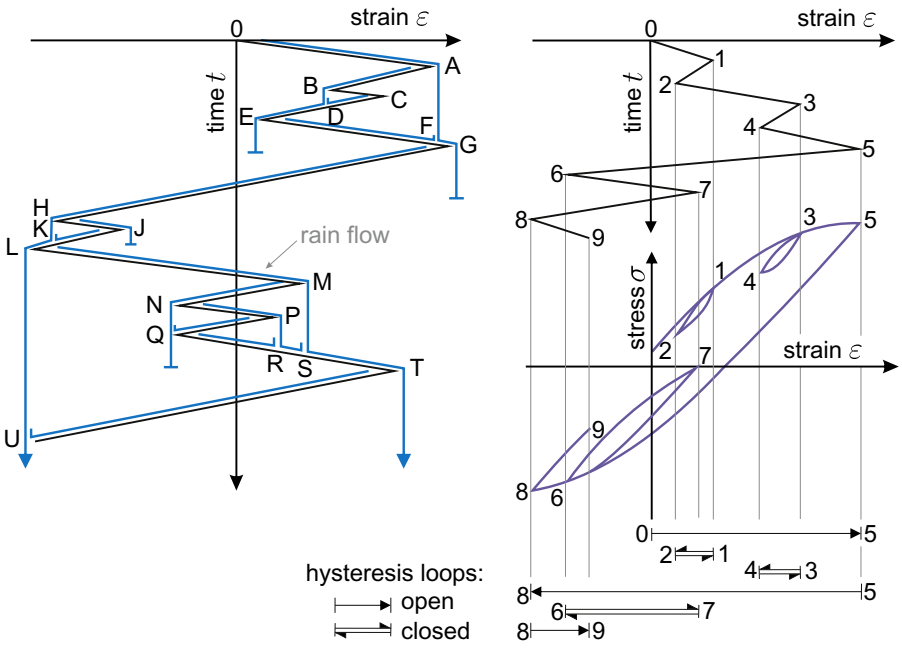

Fig. 2. Rainflow counting and its relation to hysteresis loops (after [22,34]).

α for $i \in \mathbb{N}_0$, destroys the specimen after $\mathcal{N}(\alpha,\beta) = \tilde{\mathcal{N}}(|\alpha-\beta|)$ cycles; the resulting curve is the so called S–N or Wöhler curve since the ansatz $\tilde{\mathcal{N}}(\alpha,\beta) = \kappa_1|\alpha-\beta|^{\kappa_2}$ exhibits a straight line in a log-log scale, where κ_1 and κ_2 are scaling constants. Using the Palmgren–Miner rule to identify and count cycles for an arbitrary load sequence u, such that the accumulated damage D_{ac} on the time interval $[0, \eta]$ is

$$D_{ac}(u,\eta) := \sum_{\beta<\alpha} \frac{c(u,\alpha,\beta,\eta)}{\mathcal{N}(\alpha,\beta)}, \tag{4}$$

where $c(u, \alpha, \beta, \eta)$ is the rainflow count associated to u on the time interval $[0, \eta]$[13,28,35].

According to Gorbet [8], symmetric RFC is equivalent to the variations of a Preisach hysteresis operator as given in the following proposition.

Proposition 1 (Damage equivalence [8])**.** *For an arbitrary load sequence $u \in CPM(\mathbb{R}_+)$, let $\Phi(u)$ be the Preisach operator in Eq. (3) with density function $\rho(\alpha,\beta) := -\frac{1}{2}\frac{\partial}{\partial\alpha\partial\beta}\left(\frac{1}{\mathcal{N}(\alpha,\beta)}\right)$, where $\mathcal{N}(\alpha,\beta)$ is the number of cycles to failure. Then the following equivalency holds*

$$D_{ac}(u,\eta) = |\Phi(u)|_{[0,\eta]}, \tag{5}$$

where $|\cdot|_{[0,\eta]}$ corresponds to the total variations in Eq. (1).

Remark 1. Note that Definition 2 is originally given on periodic operators [8], which we do not use here. The direct implication of this is that we do not take into account the rainflow residual in $c(u, \alpha, \beta, \eta)$, which is a fair assumption if a sufficiently large time window is considered.

Following the interpretation of RFC given in [8], symmetric rainflow counting is equivalent to the variations of the Preisach operator with density function ρ as function of $\mathcal{N}(\beta,\alpha)$. Note that by Definition 2, the density can be given in terms of the Wöhler coefficients κ_1 and κ_2 but may require a spatial discretization. The interpretation of the previous result is that the RFC method counts the number of oscillations at each range of amplitude, and this is equivalent to $|\Phi(u)|_{[0,\eta]}$, namely the number of oscillations of u between the thresholds β and α.

3. Relations of fatigue-damage accumulation and dissipated energy in hysteresis operators

In this section, we review the stored and dissipated energy properties of the Preisach hysteresis model. Subsequently, we relate dissipated energy of a class of Preisach operators to total variations and present a related notion of dissipation energy in another class of hysteresis operators, namely, the Duhem hysteresis model. Lastly, a comparison between fatigue-damage accumulation, total variations and dissipated energy is shown.

3.1. Energy dissipation property in the Preisach model

In order to shed some light into the energy characteristics in the Preisach model, we review the energy property of the atomic units (the so-called *hysterons*) of the Preisach model, which are given by relay operators with different width and mid-point. As thoroughly explained in [15], the dissipated energy of a single relay in one cycle is equal to $2\rho(\alpha,\beta)\cdot(\alpha-\beta) = q_\alpha + q_\beta$, where α and β are the up-switch and down-switch moment of the relay, respectively (see also the relay illustration in Fig. 3(c,)–(e), $q_\alpha := 2\rho(\alpha, \beta)\alpha$ and $q_\beta := -2\rho(\alpha,\beta)\beta$. Hence, the dissipated energy in one cycle for a single relay is the area of the relay, i.e., $q_\alpha + q_\beta$. The previous is sketched in Fig. 3 for a given input $u(t)$.

In the current control literature, there are two descriptions of the dissipated energy for individual relays. For the first description, when either q_α or q_β is negative for a given relay, it implies that the energy is recovered from the relay when it switches [15]. In the second one, it is assumed that the dissipated energy is split evenly between switches, such that $q_\alpha = q_\beta$ [27]. The energy storage and dissipation of individual relays for both descriptions are summarized in Table 1. We also make use of the sub-regions in

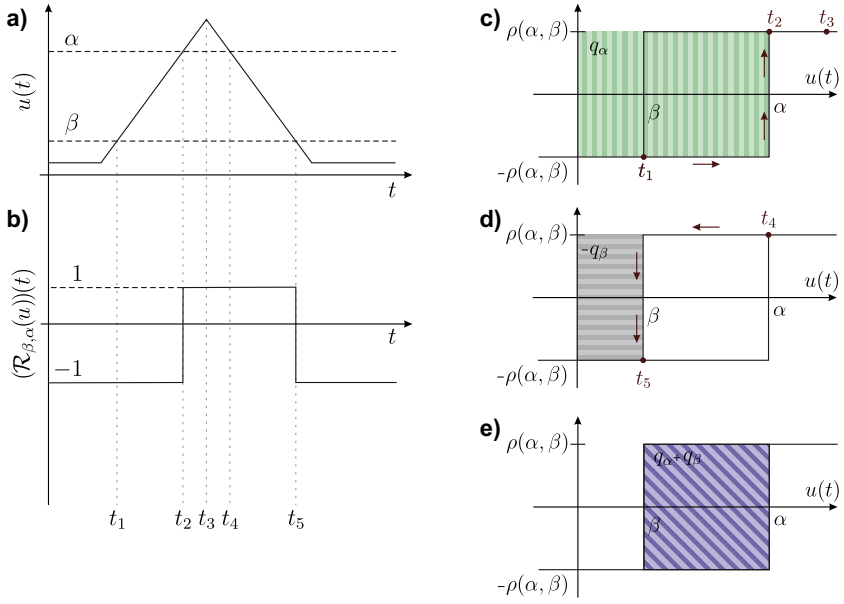

Fig. 3. Relay energy transfer for one cycle: (a) input signal, (b) relay output, (c) used energy at t_3 (q_α), (d) recovered energy at t_5 ($-q_\beta$), (e) lost or dissipated energy in one cycle ($q_\alpha + q_\beta$).

Table 1
Relays energy transfer for the Preisach model.

Sub-region of $\mathcal{P}$	Switch in relays	Stored energy as in [15]	Lost energy as in [15]	Lost energy as in [27]
$\mathcal{Q}_1$	$+1 \to -1$	$\lvert q_\beta \rvert$	0	$1/2\lvert q_\alpha + q_\beta \rvert$
$\mathcal{Q}_1$	$-1 \to +1$	0	$\lvert q_\alpha + q_\beta \rvert$	$1/2\lvert q_\alpha + q_\beta \rvert$
$\mathcal{Q}_2$	$+1 \to -1$	0	$\lvert q_\beta \rvert$	$1/2\lvert q_\alpha + q_\beta \rvert$
$\mathcal{Q}_2$	$-1 \to -1$	0	$\lvert q_\alpha \rvert$	$1/2\lvert q_\alpha + q_\beta \rvert$
$\mathcal{Q}_3$	$+1 \to +1$	0	$\lvert q_\alpha + q_\beta \rvert$	$1/2\lvert q_\alpha + q_\beta \rvert$
$\mathcal{Q}_3$	$-1 \to -1$	$\lvert q_\alpha \rvert$	0	$1/2\lvert q_\alpha + q_\beta \rvert$

the Preisach plane $\mathcal{P}$ defined as

$$\mathcal{Q}_1 := \{(\alpha,\beta) \in \mathcal{P} \mid \alpha > 0, \beta > 0\}, \tag{6a}$$

$$\mathcal{Q}_2 := \{(\alpha,\beta) \in \mathcal{P} \mid \alpha \geq 0, \beta \leq 0\}, \tag{6b}$$

$$\mathcal{Q}_3 := \{(\alpha,\beta) \in \mathcal{P} \mid \alpha < 0, \beta < 0\}. \tag{6c}$$

We consider that the relays comprising the Preisach hysteresis are divided into two time-varying sets, by fixing u, represented by the regions

$$\mathcal{P}^u_+(t) := \{(\alpha,\beta) \in \mathcal{P} \mid \big(\mathcal{R}_{\beta,\alpha}(u)\big)(t) = +1\}, \tag{7a}$$

$$\mathcal{P}^u_-(t) := \{(\alpha,\beta) \in \mathcal{P} \mid \big(\mathcal{R}_{\beta,\alpha}(u)\big)(t) = -1\}, \tag{7b}$$

such that $\mathcal{P} = \mathcal{P}^u_+(t) \cup \mathcal{P}^u_-(t)$ for every t. For notational simplicity, in the sequel we use $\mathcal{P}_+(t)$ and $\mathcal{P}_-(t)$, to refer to $\mathcal{P}^u_+(t)$ and $\mathcal{P}^u_-(t)$, respectively. For example, if u: $t \mapsto t$ then $\mathcal{P}_+(t) = \{(\alpha,\beta) \in \mathcal{P} \mid \beta < \alpha \text{ and } t < \alpha\}$. Thus, looking at Table 1 and using the sub-regions in (6) and (7), we can express the lost or dissipated energy as

$$\begin{aligned} &\iint_{\mathcal{Q}_1 \cap \mathcal{P}_-} \lvert q_\alpha + q_\beta \rvert d\alpha d\beta + \iint_{\mathcal{Q}_3 \cap \mathcal{P}_+} \lvert q_\alpha + q_\beta \rvert d\alpha d\beta \\ &+ \iint_{\mathcal{Q}_2 \cap \mathcal{P}_+} \lvert q_\beta \rvert d\alpha d\beta + \iint_{\mathcal{Q}_2 \cap \mathcal{P}_-} \lvert q_\alpha \rvert d\alpha d\beta. \end{aligned} \tag{8}$$

Alternatively, with the evenly split energy approach, the hysteretic loss is given by

$$\iint_\Omega \rho(\alpha,\beta)(\alpha - \beta) d\alpha d\beta, \tag{9}$$

where Ω is the region of points in the Preisach plane $\mathcal{P}$ for which the boundary of relays has changed during some input variation [27, p.46]. A typical shape of the region Ω is shown in Fig. 4, where the sub-regions in the Preisach plane are shown $-\mathcal{Q}_1, \mathcal{Q}_2, \mathcal{Q}_3, \mathcal{P}_+$ and $\mathcal{P}_-$— at two consequent time instances t_i and t_{i+1}. The boundary between the time-varying regions $\mathcal{P}_+$ and $\mathcal{P}_-$ is a staircase-like line whose vertices have α and β coordinates coinciding with local maxima and minima, respectively, of input at previous instants of time; the final segment of this staircase-like line is connected to the line $\alpha = \beta$ and shifts when the input signal is changed [27, p.10]. To formalize the notion of dissipated energy, we let $\Omega := \Omega_\uparrow \cup \Omega_\downarrow$, where we define the sub-regions $\Omega_\uparrow$ and $\Omega_\downarrow$ in the Preisach plane $\mathcal{P}$ whenever a switch in the relays occur from -1 to $+1$ for $\Omega_\uparrow$ and form $+1$ to -1 for $\Omega_\downarrow$ in the time interval $[t_i, t_{i+1}]$, i.e.,

$$\Omega_\uparrow := \Omega_{\uparrow[t_i,t_{i+1}]} = \mathcal{P}_-(t_i) \cap \mathcal{P}_+(t_{i+1}), \tag{10a}$$

$$\Omega_\downarrow := \Omega_{\downarrow[t_i,t_{i+1}]} = \mathcal{P}_+(t_i) \cap \mathcal{P}_-(t_{i+1}). \tag{10b}$$

Following the evenly split energy loss assumption of Mayergoyz [27], the dissipated energy between two consecutive time instances t_i and t_{i+1}, can be rewritten as

$$\begin{aligned} \mathcal{D}_{[t_i,t_{i+1}]} := \mathcal{D}^u_{[t_i,t_{i+1}]} &= \iint_{(\mathcal{Q}_1 \cup \mathcal{Q}_2 \cup \mathcal{Q}_3) \cap (\Omega_\uparrow \cup \Omega_\downarrow)} \frac{\lvert q_\alpha + q_\beta \rvert}{2} d\alpha d\beta, \\ &= \iint_{\mathcal{P} \cap (\Omega_\uparrow \cup \Omega_\downarrow)} \frac{2\rho(\alpha,\beta)(\alpha - \beta)}{2} d\alpha d\beta \\ &= \iint_{\Omega_{[t_i,t_{i+1}]}} \rho(\alpha,\beta)(\alpha - \beta) d\alpha d\beta, \end{aligned} \tag{11}$$

which brings us back to Eq. (9) for a time interval $[t_i, t_{i+1}]$. In the following proposition we consider the dissipated energy on an interval $[0, \eta]$ given by $\mathcal{D}_{[0,\eta]} : u \mapsto \mathcal{D}^u_{[0,\eta]}$, being of special interest due to its connection to damage.

Proposition 2 (Dissipation equivalence). *Let input $u \in CPM(\mathbb{R}_+)$. Consider the Preisach hysteresis operator Φ_1 defined as in Eq. (3) and a Preisach hysteresis operator $\Phi_2(u)$ with density function $\hat{\rho}(\alpha,\beta) = \frac{2\rho(\alpha,\beta)}{\alpha-\beta} = -\frac{\partial}{\partial\alpha}\frac{\partial}{\partial\beta}\left(\frac{1/\mathcal{N}(\alpha,\beta)}{\alpha-\beta}\right)$, where $\mathcal{N}(\alpha,\beta)$ is the*

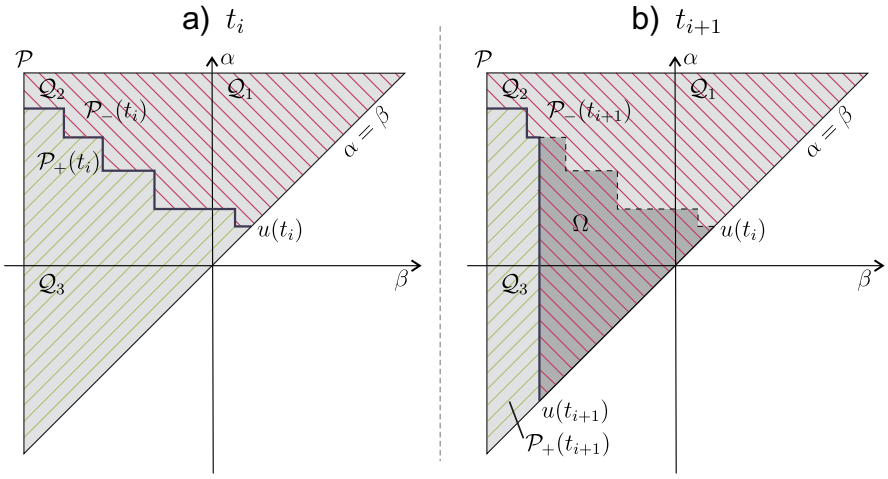

Fig. 4. Preisach plane $\mathcal{P}$, the Ω region, and the sub-regions $\mathcal{P}_+$, $\mathcal{P}_-$, $\mathcal{Q}_1$, $\mathcal{Q}_2$ and $\mathcal{Q}_3$ for a) t_i and b) t_{i+1}.

number of cycles to failure. Then it follows that

$$D_{ac}(u,\eta) = \mathcal{D}_{[0,\eta]}\big(\Phi_2(u)\big) + c_1, \tag{12}$$

where c_1 is the initial condition of $\Phi_1(u)$.

The proof of this proposition can be found in the Appendix. From Propositions 1 and 2, we have established the direct relation between the damage accumulation and the material dissipated energy through a class of Preisach hysteresis operator. In [8], the dissipated energy is also described in terms of variations of certain Preisach hysteresis operator for rheological models. However, here we have related dissipation directly to fatigue-damage accumulation, by means of the interpretation of the Ω region. Relating dissipation to fatigue-damage could be thought of as a matter of scaling in the density function.

3.2. Energy dissipation in the Duhem model

As discussed in the Introduction, the Duhem models describe very well physical phenomena such as magnetics and friction. This implies that we can use them for approximating the fatigue-damage accumulation in electromechanical systems, as an alternative to the use of the infinite-dimensional Preisach models. We will also rely on the well-developed dissipative systems theory in [42].

The Duhem hysteresis model is described by a non-smooth differential equation where the rate of change of its state variable switches according to the input velocity [26]. It has a scalar memory, i.e., it accesses information about past evolution through a single state variable at each time, in contrast to the Preisach model that exhibits infinite dimensional memory [8]. Using the same description as in [26,31,41] the Duhem operator $\Phi : AC(\mathbb{R}_+) \times \mathbb{R}_+ \to AC(\mathbb{R}_+)$, $(u, y_0) \mapsto \Phi(u, y_0) =: y$ is described by

$$\dot{y}(t) = f_1\big(y(t),u(t)\big)\dot{u}_+(t) + f_2\big(y(t),u(t)\big)\dot{u}_-(t), \quad y(0) = y_0, \tag{13}$$

where $\dot{u}_+(t) := \max\{0, \dot{u}(t)\}$, $\dot{u}_-(t) := \min\{0, \dot{u}(t)\}$ and f_1 and f_2 are continuously differentiable functions.

As discussed in [30], the hysteretic phenomenon can be classified according to its input-output mapping into counter-clockwise (CCW), clockwise (CW) or more complex behavior. In particular, the Preisach operator can exhibit either CCW or CW dynamics, depending on the weights used on the individual relays composing the model. According to Gorbet [8], the strain-stress constitutive law with stress as input and strain output gives rise to CCW loops. Hence, since we are interested in such relationships we will consider the CCW case in the Duhem model in the sequel.

Definition 3 (Duhem CCW dissipativity ineq.)**.** The Duhem operator as in Eq. (13) is said to be dissipative with respect to the supply rate $\dot{y}u$ if there exists a non-negative function $H : \mathbb{R}^2 \to \mathbb{R}_+$ such that for every $u \in AC(\mathbb{R}_+)$ and $y_0 \in \mathbb{R}$

$$\frac{dH\big(y(t),u(t)\big)}{dt} \le \dot{y}(t)u(t) \tag{14}$$

holds for almost all $t \in \mathbb{R}_+$ with $y := \Phi(u, y_0)$.

If we consider H as defined in Definition 3 as being the stored energy in the system, the inequality in Eq. (14) can be interpreted as the exchange of energy with the environment where the supplied energy given by $\int_0^T \dot{y}(\tau)u(\tau)d\tau$ is subtracted by a non-negative quantity, which we refer to as the dissipated energy. Examples on how to explicitly construct such H can be found in [29].

Definition 4 (Duhem CCW Dissipated energy)**.** For the Duhem hysteresis operator Φ with $y = \Phi(u)$, the dissipated energy $\mathcal{D} : AC(\mathbb{R}_+) \times AC(\mathbb{R}_+) \to AC(\mathbb{R}_+)$ for the CCW case is defined by

$$\mathcal{D}_{[0,t]}(y,u) = \int_0^t \dot{y}(\tau)u(\tau)d\tau - H\big(y(t),u(t)\big) + H\big(y(0),u(0)\big). \tag{15}$$

It is immediate to check that $\dot{\mathcal{D}}_{[0,t]}(y,u) \ge 0$ for all t, or in other words the dissipated energy is a non-decreasing function along the trajectory of y and u. Note that this property is also valid for the damage function and dissipated energy of the Preisach model as discussed before.

3.3. Comparison

Since the Preisach and Duhem models are both phenomenological models of hysteresis, the interpretation of dissipated energy as damage accumulation in the Preisach model can be carried over to the Duhem one. For example, in [7] a Duhem model is used to approximate the same phenomenon that has been widely described using the Preisach model. In particular, the Duhem model Φ in Eq. (13) can approximate the Preisach model Φ_2 such that the corresponding dissipated energy $\mathcal{D}_{[0,t]}(y,u)$ in Eq. (15) approximates the damage accumulation $D_{ac}(u,\eta)$ in Eq. (4).

At the top of Fig. 5, an example of a wind turbine tower bending moment M_t with a duration of $T = 600$s is presented. At the bottom of Fig. 5, a comparison among the normalized accumulated damage in the RFC sense, the variations of a Preisach hysteresis, and the dissipated energy of a Duhem hysteresis are shown. The aim of this comparison is to show that the dissipated energy of

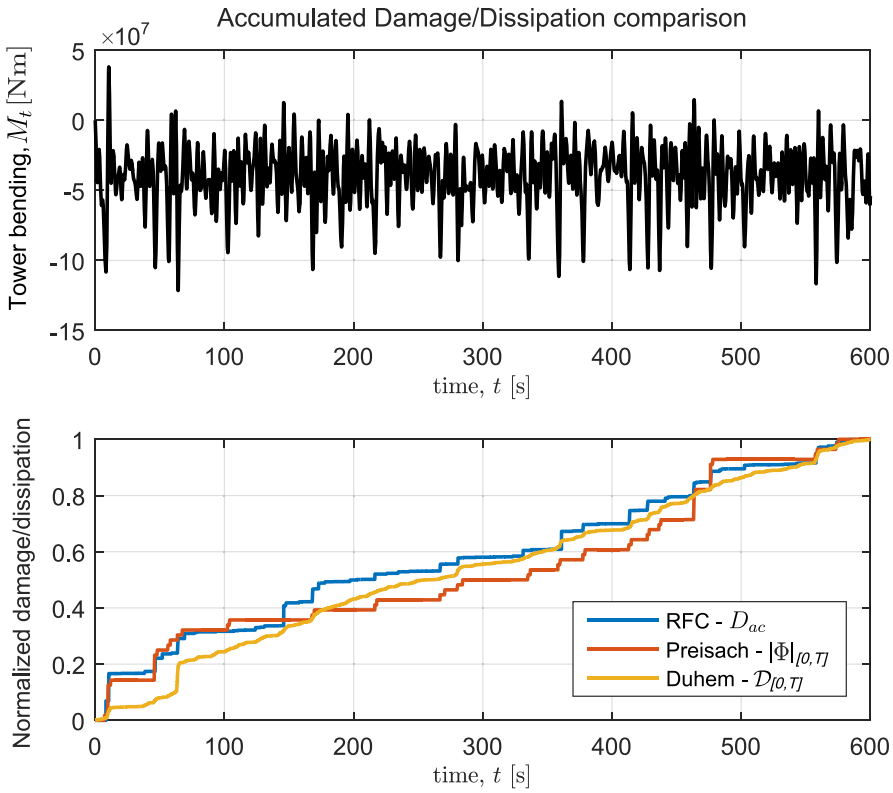

Fig. 5. Comparison of accumulated damage in the RFC sense, variations of an approximated Preisach hysteresis operator and dissipated energy of a Duhem hysteresis operator.

the Duhem hysteresis operator $\mathcal{D}_{[0,T]}$ in (15) can approximate the accumulated damage D_{ac} in (4). The accumulated damage $D_{ac}(M_t, T)$ was calculated using coeffcients κ_1 and κ_2 corresponding to B1 steel with the toolbox from [28]. The variations of the Preisach operator $|\Phi(M_t)|_{[0,T]}$ were approximated using a weighted sum of three relays. Lastly, the dissipated energy of the Duhem hysteresis model $\mathcal{D}_{[0,T]}(y, M_t)$ was calculated for a Duhem hysteresis semi-linear model for the CCW case; this model will be discussed in further detail in Section 4.2.

4. Fatigue-damage minimization model predictive control strategy

In the previous sections, we have established the relation between the fatigue-damage accummulation in the RFC sense to the energy dissipation property of hysteresis operators. In this section, using a well-studied wind-turbine model, we embed the dissipated energy as a fatigue-damage proxy or surrogate in the model predictive control (MPC) problem formulation. Firstly, we discuss the plant dynamics for the prediction model in Section 4.1. It is followed by the approximation of fatigue-damage accumulation using a Duhem hysteresis semi-linear model in Section 4.2. Subsequently, we present a modified MPC strategy in Section 4.3, where we include the dissipated energy in the cost functional, as a means to penalize the fatigue-damage accumulation in a certain component of the electromechanical system, which in this case is the shaft. We show the efficacy of the proposed method in simulation results.

4.1. Wind turbine dynamics

Consider the tip speed ratio a rational function defined as $\lambda(\omega_r, v) := R_r\omega_r/v$, where R_r is the rotor radius, ω_r is the rotor angular speed, and v corresponds to the effective wind speed at the rotor. The wind turbine rotor extracts mechanical power from the wind and is given by

$$P_r(\lambda, \beta_p) = \frac{\pi}{2}\rho_a R_r^2 v^3 C_P(\lambda, \beta_p), \tag{16}$$

where C_P represents the aerodynamic efficiency in terms of the collective blade pitch angle β_p and ρ_a stands for the air density.

For controller design purposes, we consider the rotational mode of the shaft, described by the following set of differential equations

$$J_r\dot{\omega}_r = T_r(\lambda, \beta_p) - K_\theta\theta - B_\theta\dot{\theta}, \tag{17a}$$

$$J_g\dot{\omega}_g = -T_g + \frac{K_\theta}{N_g}\theta + \frac{B_\theta}{N_g}\dot{\theta}, \tag{17b}$$

$$\dot{\theta} = \omega_r - \frac{\omega_g}{N_g}, \tag{17c}$$

where ω_r corresponds to the rotor angular velocity, ω_g to the generator angular velocity, and θ to the shaft torsion. Furthermore, N_g stands for the gear ratio, T_g is the generator torque and $T_r(\lambda, \beta_p) = P_r(\lambda, \beta_p)/\omega_r$ is the aerodynamic rotor torque. The rotor and generator inertias are J_r and J_g, respectively, and the drive-train stiffness and damping are described by the coefficients K_θ and B_θ, respectively. This model is sketched in Fig. 6. Here we assume perfect measurement of the shaft torsion.

Discretizing and linearizing the model in Eq. (17) with a chosen sampling time T_s around an operating point for a chosen mean wind speed, the following DLTI system is obtained

$$x_{k+1} = A_d x_k + B_d u_k + E_d d_k, \tag{18}$$

where the state vector is given by $x_k = (\omega_{g,k}, \omega_{r,k}, \theta_k)$, and the vector of inputs or controls is given as $u_k = (\beta_{p,k}, T_{g,k})$. Lastly, the residual of the wind speed is considered as an unknown disturbance such that $d_k = v_k$. The system parameters from Eq. (17) are

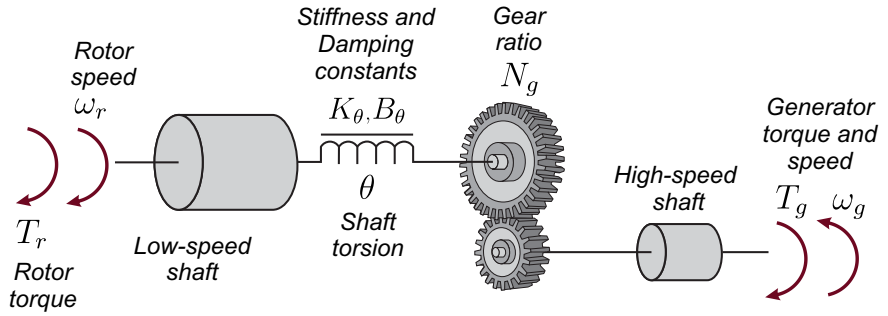

Fig. 6. Wind turbine simplified drive-train model.

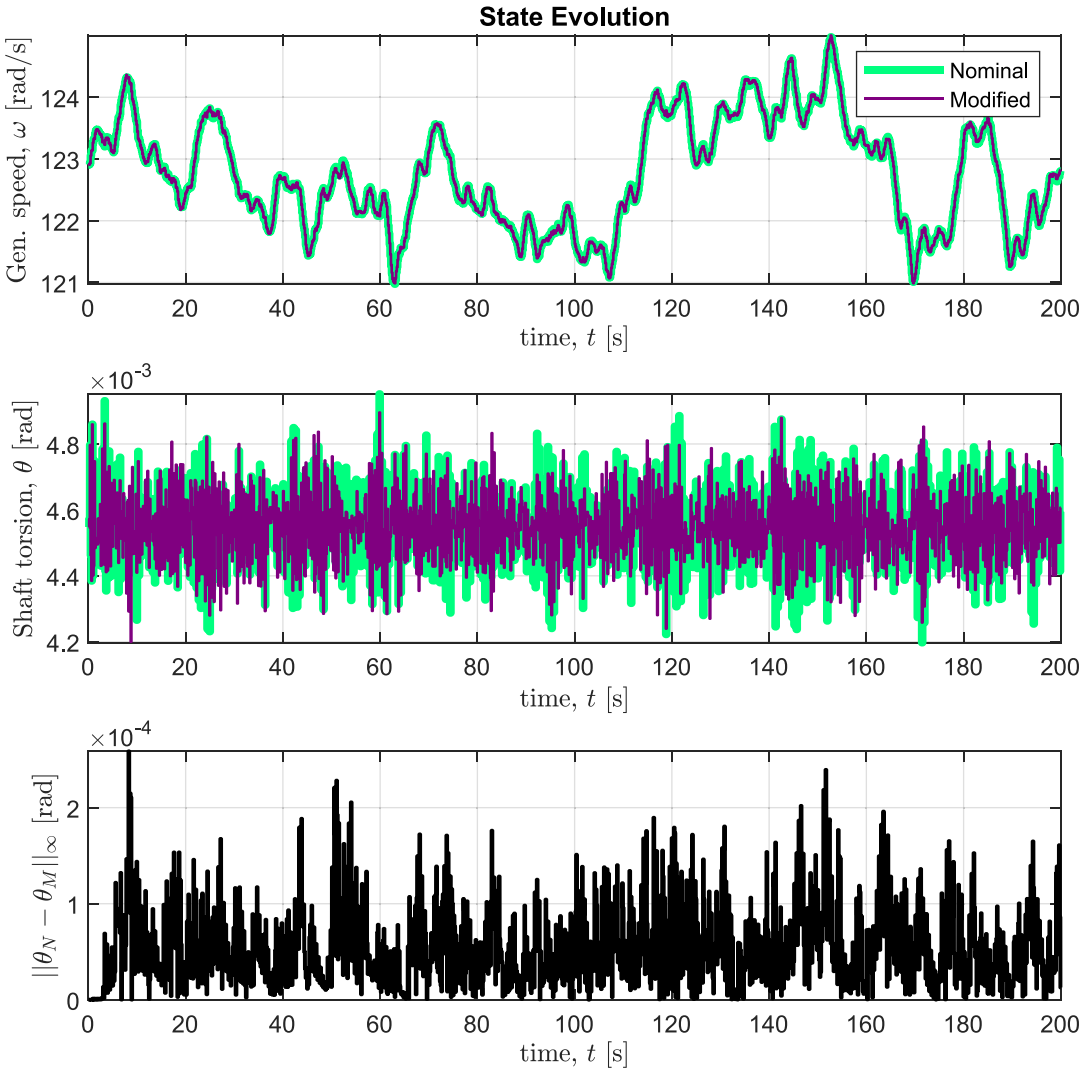

Fig. 7. Selected states evolution and norm between both strategies shaft torsion.

taken from Pour et al. [21] after linearizing around a chosen operating point.

Furthermore, we use the state selector C such that

$$z_k = \begin{bmatrix} 0 & 0 & 1 \end{bmatrix} x_k = C x_k = \theta_k, \tag{19}$$

is the input to the Duhem hysteresis operator such that $y = \Phi(z)$. Hence, we see the shaft torsion $z = \theta$ as the stress input and y as the strain output. In the sequel, we use the dissipated energy of this Duhem model as a proxy of the damage in the shaft.

4.2. Duhem semi-linear model

As mentioned before, the Duhem model can be explicitly written down as a differential equation. In this paper, we consider the Duhem semi-linear model [32], where the Duhem operator $y = \Phi(z)$ is governed by

$$\dot{y} = (\bar{\gamma}_1 y + \bar{\mu}_1 z)\dot{z}_+ + (\bar{\gamma}_2 y + \bar{\mu}_2 z)\dot{z}_-, \tag{20}$$

with $\dot{z}_+ := \max\{0, \dot{z}\}$, $\dot{z}_- := \min\{0, \dot{z}\}$, and $\bar{\gamma}_1, \bar{\gamma}_2, \bar{\mu}_1, \bar{\mu}_2$ being parameters that characterize the stress-strain behavior. The semi-linear Duhem hysteresis model in Eq. (20) can also be expressed

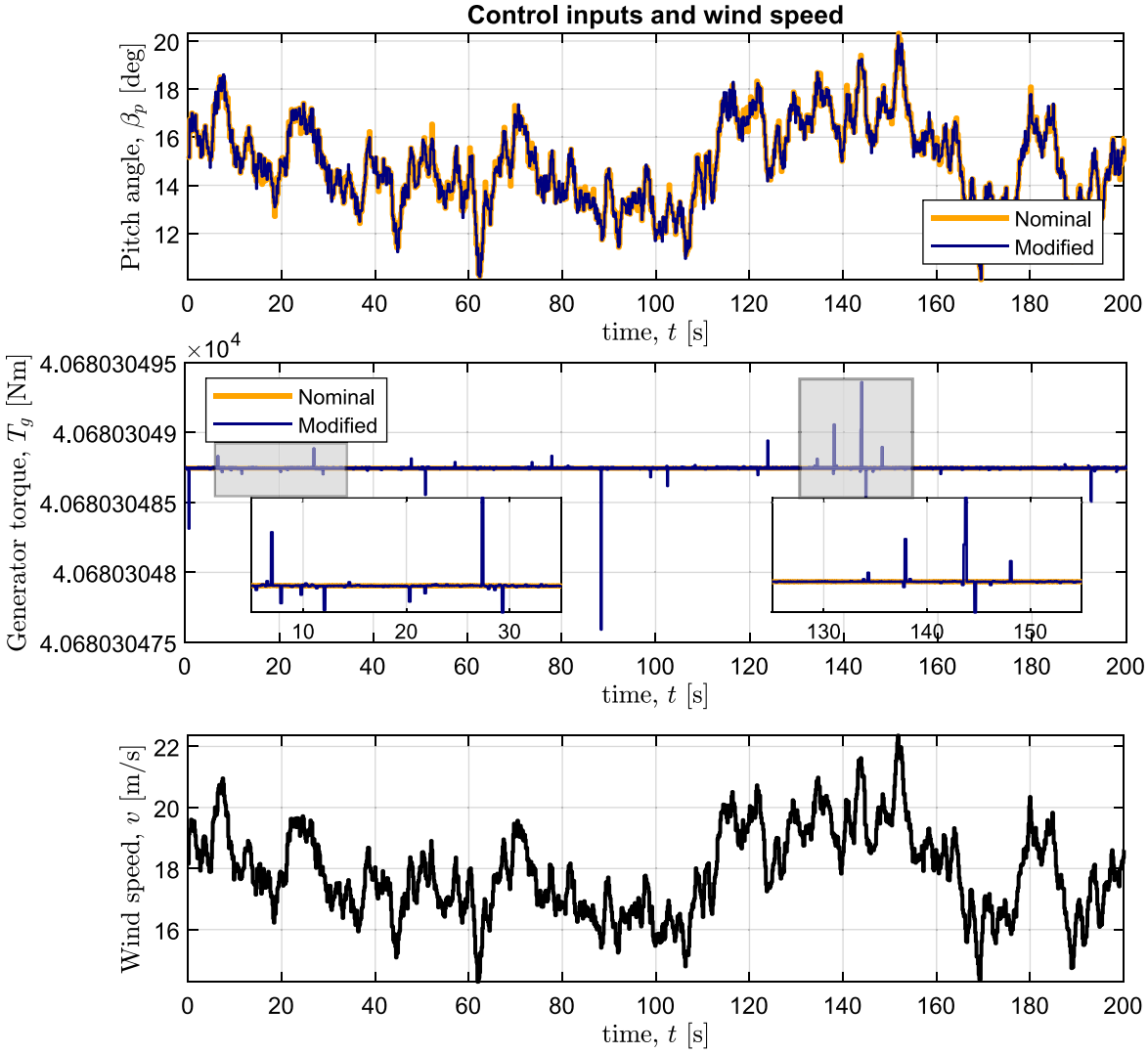

Fig. 8. Collective pitch angle, generator torque and wind disturbance.

as the switched system

$$\dot{y} = \begin{cases} (\bar{\gamma}_1 y + \bar{\mu}_1 z)\dot{z}, & \text{if } \dot{z} \geq 0, \\ (\bar{\gamma}_2 y + \bar{\mu}_2 z)\dot{z}, & \text{if } \dot{z} \leq 0. \end{cases} \tag{21}$$

Using the Euler discretization with sampling time T_s, the differential equation in Eq. (21) can be rewritten as

$$y_{k+1} - y_k = \begin{cases} (\gamma_1 y_k + \mu_1 z_k)(z_{k+1} - z_k), & \text{if } z_{k+1} - z_k \geq 0, \\ (\gamma_2 y_k + \mu_2 z_k)(z_{k+1} - z_k), & \text{if } z_{k+1} - z_k \leq 0, \end{cases} \tag{22}$$

with $\gamma_1 = \bar{\gamma}_1 T_s$, $\mu_1 = \bar{\mu}_1 T_s$, $\gamma_2 = \bar{\gamma}_2 T_s$ and $\mu_2 = \bar{\mu}_2 T_s$.

4.3. Model predictive control problem formulation

Model predictive control (MPC) is an optimization based control strategy that handles both complex systems and constraints; the idea behind MPC is to predict the state evolution since the system dynamics are known, and it effectively solves a constrained optimal control problem [9,25]. Several damage reduction MPC based strategies for wind turbine control have been proposed, for example in [2,4,38]. The intention here is to make use of the dissipated energy in Eq. (15) as a proxy or surrogate for accumulated damage in the shaft. We use the observation that z and y are bounded and H is continuous; hence, for sufficiently large time T, the primary contribution in dissipation is due to the supply rate, and thereby we can approximate Eq. (15) by the integral of the supply rate

$$\begin{aligned} \mathcal{D}_{[0,T]}(y,z) &\approx \int_0^T \dot{y}(t)z(t)dt = y(t)z(t)\Big|_0^T - \int_0^T y(t)\dot{z}(t)\,dt, \\ &= y(T)z(T) - y(0)z(0) - \int_0^T y(t)\dot{z}(t)\,dt, \end{aligned} \tag{23}$$

which after discretizing yields

$$\begin{aligned} \mathcal{D}_{[0,N\cdot T_s]}(y,z) &= y_N z_N - y_0 C z_0 - \sum_{k=0}^{N-1} y_k z_{k+1} \\ &= y_N C x_N - y_0 C z_0 - \sum_{k=0}^{N-1} y_k (CA_d x_k + CB_d u_k), \end{aligned} \tag{24}$$

where we used $z_k = Cx_k$ and $z_{k+1} = Cx_{k+1}$. Subsequently, we propose a cost functional composed of a standard running cost and terminal state cost, augmented with the running cost of the discretized dissipated energy in Eq. (24), such that

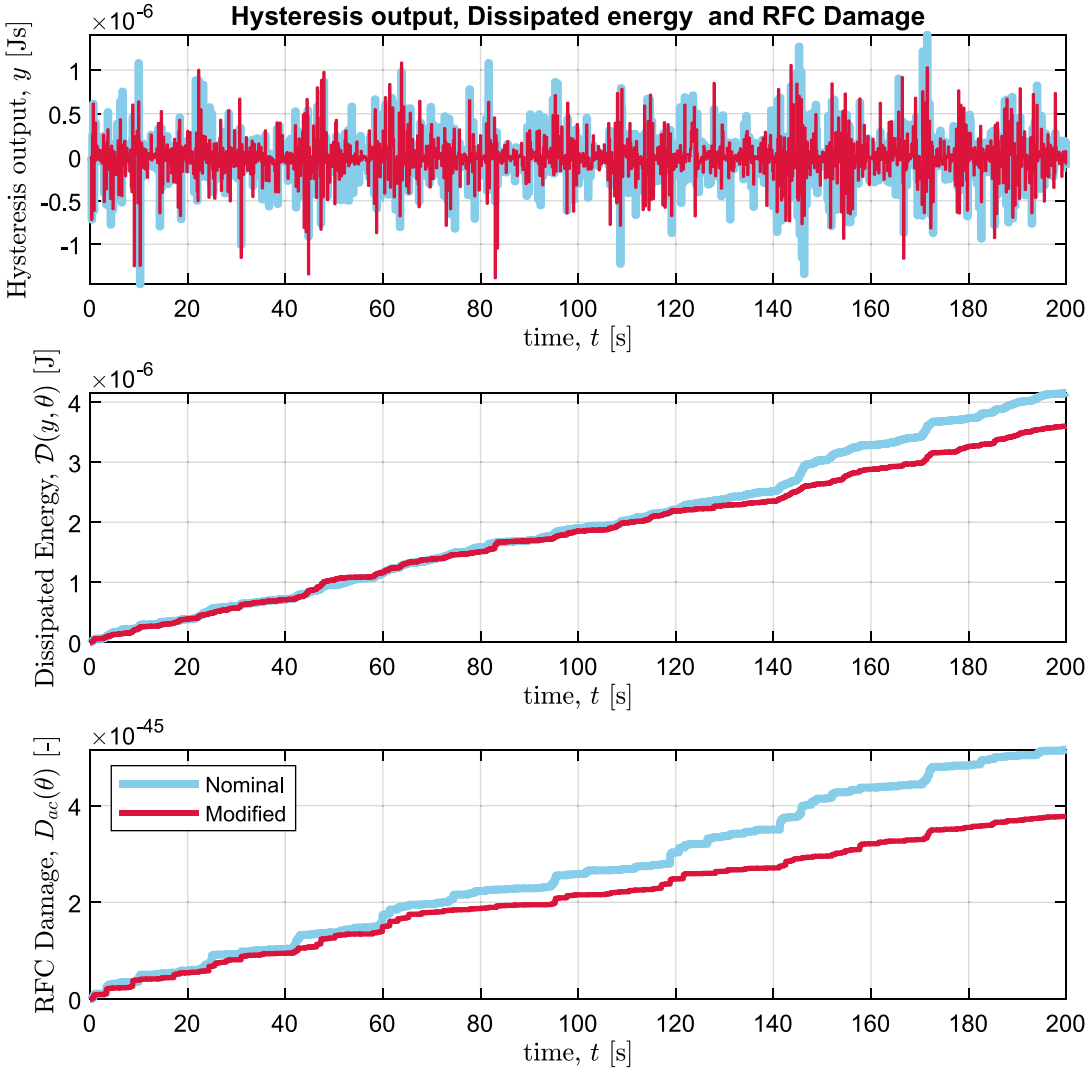

Fig. 9. Hysteresis output, dissipated energy and accumulated RFC damage.

$$J(y,x,u)=\sum_{k=0}^{N-1}\left(x_k^\top Q x_k+u_k^\top R u_k\right)+x_N^\top Q_f x_N + \sum_{k=0}^{N-1} y_k^\top W y_k-\sum_{k=0}^{N-1} y_k W C A_d x_k-\sum_{k=0}^{N-1} y_k W C B_d u_k. \tag{25}$$

In order to guarantee positiveness of the cost functional in Eq. (25), we rewrite it in matrix form as

$$\Xi:=\begin{bmatrix} Q & 0 & -1/2WCA_d \\ 0 & R & -1/2WCB_d \\ (-1/2WCA_d)^\top & (-1/2WCB_d)^\top & W \end{bmatrix} \tag{26}$$

where $Q=Q^\top\succ 0$, $R=R^\top\succ 0$ and $W>0$ such that $\Xi\succ 0$ and $Q_f=Q_f^\top\succ 0$ for the terminal cost.

Consequently, we can cast the modified damage reduction MPC strategy in discrete time, where we include the penalty on the shaft damage as

$$\min_U J:=\sum_{k=0}^{N-1}\begin{bmatrix}x_k\\u_k\\y_k\end{bmatrix}^\top \Xi\begin{bmatrix}x_k\\u_k\\y_k\end{bmatrix}+x_N^\top Q_f x_N \tag{27a}$$

$$s.t.\begin{cases} x_0=x(t),\\ x_{k+1}=A_d x_k+B_d u_k, \text{ for } k=0,1,\dots,N-1,\\ x_{\min}\le x_k\le x_{\max}, \text{ for } k=1,\dots,N,\\ u_{\min}\le u_k\le u_{\max}, \text{ for } k=0,1,\dots,N,\\ y_0=y(t),\\ y_{k+1}=\begin{cases} y_k+(\gamma_1 y_k+\mu_1)(z_{k+1}-z_k), & \text{if } z_{k+1}-z_k\ge 0,\\ y_k+(\gamma_2 y_k+\mu_2)(z_{k+1}-z_k), & \text{if } z_{k+1}-z_k<0,\end{cases}\\ \qquad\qquad \text{for } k=0,1,\dots,N-1, \end{cases} \tag{27b}$$

over $U:=\{u_0,\dots,u_N\}$, for a horizon $N\in\mathbb{N}$, and weights $Q=Q^\top\succ 0$, $R=R^\top\succ 0$, $W>0$, and $Q_t=Q_t^\top\succ 0$. Note that $z_{k+1}=Cx_{k+1}$ in Eq. (27b) can be expressed in terms of x_k and u_k.

Note that through the weighting matrix Ξ in (26) the cost functional or objective function $J(y, x, u)$, the MPC formulation considers penalization on the states, the control inputs and the strain in the shaft given by $y=\Phi(\theta)$. Therefore, since θ is encompassed in the state vector and the hysteresis evolution has been included in the dynamics in (27b), it can be seen that the dissipated energy $\mathcal{D}(y,\theta)$ in (23) has been embedded in the modified MPC strategy (27). In the following, the simulations illustrating this control strategy are presented with the objective of showing the impact on both dissipated energy and accumulated damage in the shaft.

Table 2
Controller computational time statistics.

Metric	Nominal MPC	Modified MPC
Min.	0.0057s	0.0445s
Max.	0.2729s	0.9838s
Mean	0.0095s	0.2189s
Std.Dev.	0.0107s	0.1342s

4.4. Simulation results

The proposed damage reduction MPC strategy was implemented in `Matlab`. The wind turbine model is a non-linear model based on the standard NREL 5MW wind turbine [21] implemented in `Simulink`, driven to the operating point of a mean wind speed of 18m/s. The model considers tower dynamics and aerodynamics, as well as the rotational mode of the shaft used in the controller synthesis, which is of particular interest here. The control strategy was implemented using `Yalmip` [23] with a sampling time of $T_s = 0.15$s. The wind is seen as a disturbance $d = v$ and was taken from wind series data; the initial conditions were set to the operating point. We chose a horizon $N = 5$ and the weights on the running cost according to Bryson's rule [14, p.537] such that Q and R are diagonal matrices with elements $(1/30^2,\ 1/0.3^2,\ 1/0.001^2)$ and $(1/30^2,\ 1/0.1^2)$, respectively; we let $W = 2.8 \times 10^{-4}$ guaranteeing $\Xi \succ 0$ in Eq. (26) and $Q_t = 100Q$. The limits on inputs and states are given as $u_{\max} = [90^\circ, 40, 700\text{Nm}]$, $u_{\min} = [0^\circ, 40, 660\text{Nm}]$, $x_{\max} = [142.9\text{rad/s}, 2.27\text{rad/s}, 8.5 \times 10^{-3}\text{rad}]$ and $x_{\min} = [102.9\text{rad/s}, 0.27\text{rad/s}, 0.5 \times 10^{-3}\text{rad}]$. For the Duhem semi-linear model in Eq. (21) the initial condition was set to $y_0 = 0$, and the coefficients were chosen as $\bar{\gamma}_1 = -1, \bar{\gamma}_2 = 1, \bar{\mu}_1 = b$, and $\bar{\mu}_2 = -b$ with $b = 20$ following [32] for the CCW case, according to stress-strain behavior.

The simulation results are presented in Figs. 7–9, where the proposed strategy in Eq. (27) is compared against a nominal one, i.e., an MPC strategy without the dissipated energy penalization and consequently without the Duhem hysteresis dynamics in the constraints. A comparison of the generator speed ω_g and the shaft torsion θ for both cases is given in Fig. 7; additionally, the pointwise infinity norm of the difference in the shaft torsion of both cases is also given, where it can be observed that the modified strategy reduces the amplitude in the shaft torsion. The inputs (β_p, T_g and v) are compared in Fig. 8, where it can be observed that the pitch angle follows the wind profile that is perceived as a disturbance by the controller. The controller computational time was calculated and the statistics are shown in Table 2 to illustrate the computational penalty incurred by adding the Duhem hysteresis dynamics in the constraints and the dissipated energy penalty in (27), being roughly 20 times more computationally expensive than the nominal controller; in here, the comparison is only for the controller computation, based on the `tic-toc` calculation per optimization step using a regular quadcore PC. Lastly, the semi-linear Duhem hysteresis output y and its respective cumulative dissipated energy $\mathcal{D}(y, \theta)$ are depicted in Fig. 9, where we can observe that the proposed strategy in Eq. (27) effectively reduces the variations in y, as well as the accumulated dissipated energy $\mathcal{D}(y, \theta)$. Moreover, the proposed control strategy is compared against the nominal strategy in the context of RFC to validate our results using the toolbox from [28]; the resulting accumulated damage curves corresponding to the the shaft $D_{ac}(\theta)$ are shown at the bottom of Fig. 9 for material coefficients corresponding to steel, i.e., intercept of log N axis of $\kappa_1 = 6.25 \times 10^{30}$ and negative inverse $S - N$ curve slope of $\kappa_2 = 4$.

From the simulation results, we conclude that embedding the dissipated energy in the shaft effectively reduces the accumulated damage in the RFC sense, alas increasing substantially the computational cost. In addition, this case study could also be extended by including a wind speed estimator [39] or wind measurement such as LIDAR [38], both of which could potentially bring further improvements by not treating wind directly as a disturbance.

5. Conclusions

Since it is not straightforward to include directly RFC into MPC formulations, in this paper, we have proposed a modified MPC strategy that uses the dissipated energy of a Duhem hysteresis model as a measure of damage in lieu of RFC. In other words, the dissipated energy of the Duhem model is embedded in the MPC problem formulation, on account of it being a numerically-tractable operator that can be explicitly written as a differential equation. In order to explain our usage of the Duhem dissipated energy as a fatigue damage model, we first showed the relationship between damage in the RFC sense and the total variations of a Preisach hysteresis operator following existing results. Subsequently, we related the dissipation in the Preisach model to total variations and once this link was established, it enabled us to make the relationship between damage and dissipation. We then transported the notion of dissipation as damage to the Duhem framework, which we eventually embedded in the MPC formulation.

Due to the infinite dimensional memory characteristic of the Preisach model, it is not straightforward to include this operator in the MPC formulation. Therefore, we approximated it with the Duhem model, which is numerically-tractable, due to the fact that both models provide a phenomenological relationship of strain-stress. We illustrated this link with an example, but it still remains to show how well the Duhem dissipation approximates the Preisach dissipation. The direct relationship between RFC and Duhem operators is something that is worth looking at, where for example, a variational system may be used to study the oscillations in the Duhem model.

We provided an application example based on NREL's 5MW wind turbine, where we illustrate the applicability of the proposed control strategy, which incorporates the dissipated energy as a damage proxy and shows a successful reduction in both. Even though we used a wind turbine example, such a strategy could be used for several other applications where fatigue damage needs to be reduced; this is also one of the advantages provided by the Duhem modeling framework. Furthermore, embedding a fatigue model in the MPC strategy, as proposed in this paper, has advantages as well as disadvantages when compared against a regular MPC without the fatigue model. On one hand, the advantages are the inclusion of the damage reduction metric directly in the cost function, and the ability to combine the damage proxy with the plant dynamics in the predictions; thus, the post-processing is not necessary. On the other hand, the disadvantages are the added computational complexity, and the fact that the model quality needs to be good in order to have accurate predictions; the latter which could potentially be improved by using knowledge on the disturbances. Lastly, the trade-off between damage reduction and increased computational time can be balanced by suitably choosing the balance weights and the horizons depending on computational resources availability; the computational cost of the modified MPC strategy could be reduced by using a dedicated solver for non-linear optimization problems.

Acknowledgments

This work was partially supported by the Danish Council for Strategic Research (contract no. 11–116843) within the 'Programme Sustainable Energy and Environment', under the "EDGE" (Efficient Distribution of Green Energy) project.

Appendix A. Proof of Proposition 2

The proof is carried out by induction, so first we prove

$$|\Phi_1(u)|_{[t_0,t_1]} - \left|\big(\Phi_1(u)\big)(t_0)\right| = \mathcal{D}_{[t_0,t_1]}\big(\Phi_2(u)\big). \tag{A.1}$$

Using the definition of total variations in Eq. (1) we compute the variations $\Phi_1(u)$ for the interval $[t_0, t_1]$, i.e.,

$$\begin{aligned}|\Phi_1(u)|_{[t_0,t_1]} &= \left|\big(\Phi_1(u)\big)(t_0)\right| + \left|\big(\Phi_1(u)\big)(t_1) - \big(\Phi_1(u)\big)(t_0)\right| \\ &= \left|\big(\Phi_1(u)\big)(t_0)\right| + \int_{\beta<\alpha} \rho(\alpha,\beta)\Big|\big(\mathcal{R}_{\beta,\alpha}(u)\big)(t_1) \\ &\quad - \big(\mathcal{R}_{\beta,\alpha}(u)\big)(t_0)\Big| d\alpha d\beta, \end{aligned} \tag{A.2}$$

where we exploited the piecewise monotonicity of $\Phi_1(u)$ and of $\mathcal{R}_{\beta,\alpha}(u)$ to get the absolute value inside the integral. The intention is to find the relationship between the variations and the dissipated energy in the Preisach model given in Eq. (11). Hence, there are only four possibilities to evaluate Eq. (A.2):

$$\begin{aligned}&\text{(i) } \big(\mathcal{R}_{\beta,\alpha}(u)\big)(t_1) = -1, \big(\mathcal{R}_{\beta,\alpha}(u)\big)(t_0) = -1 \\ &\quad \to \left|\big(\mathcal{R}_{\beta,\alpha}(u)\big)(t_1) - \big(\mathcal{R}_{\beta,\alpha}(u)\big)(t_0)\right| = 0, \end{aligned} \tag{A.3a}$$

$$\begin{aligned}&\text{(ii) } \big(\mathcal{R}_{\beta,\alpha}(u)\big)(t_1) = -1, \big(\mathcal{R}_{\beta,\alpha}(u)\big)(t_0) = 1 \\ &\quad \to \left|\big(\mathcal{R}_{\beta,\alpha}(u)\big)(t_1) - \big(\mathcal{R}_{\beta,\alpha}(u)\big)(t_0)\right| = 2, \end{aligned} \tag{A.3b}$$

$$\begin{aligned}&\text{(iii) } \big(\mathcal{R}_{\beta,\alpha}(u)\big)(t_1) = 1, \big(\mathcal{R}_{\beta,\alpha}(u)\big)(t_0) = -1 \\ &\quad \to \left|\big(\mathcal{R}_{\beta,\alpha}(u)\big)(t_1) - \big(\mathcal{R}_{\beta,\alpha}(u)\big)(t_0)\right| = 2, \end{aligned} \tag{A.3c}$$

$$\begin{aligned}&\text{(iv) } \big(\mathcal{R}_{\beta,\alpha}(u)\big)(t_1) = 1, \big(\mathcal{R}_{\beta,\alpha}(u)\big)(t_0) = 1 \\ &\quad \to \left|\big(\mathcal{R}_{\beta,\alpha}(u)\big)(t_1) - \big(\mathcal{R}_{\beta,\alpha}(u)\big)(t_0)\right| = 0. \end{aligned} \tag{A.3d}$$

From the previous we can conclude that Eq. (A.2) will only yield non-zero values when a switch in the relays occur, i.e., for cases Eq. (A.3b) and Eq. (A.3c) the variations in Eq. (A.2) become

$$|\Phi_1(u)|_{[t_0,t_1]} = \left|\big(\Phi_1(u)\big)(t_0)\right| + \iint_{\Omega_{[t_0,t_1]}} 2\rho(\alpha,\beta) d\alpha d\beta. \tag{A.4}$$

Let $c_1 = \left|\big(\Phi_1(u)\big)(t_0)\right|$. On the other hand, following Eq. (11), the dissipated energy of the weighted Preisach hysteresis operator $\Phi_2(u)$ is given by

$$\begin{aligned}\mathcal{D}_{[t_0,t_1]}\big(\Phi_2(u)\big) &= \iint_{\Omega_{[t_0,t_1]}} \hat{\rho}(\alpha,\beta)(\alpha-\beta) d\alpha d\beta \\ &= \iint_{\Omega_{[t_0,t_1]}} 2\rho(\alpha,\beta) d\alpha d\beta = |\Phi_1(u)|_{[t_0,t_1]} - c_1. \end{aligned} \tag{A.5}$$

Hence, Eq. (12) holds for the first step. Notice that if one uses the definition in Eq. (1) then Eq. (A.5) is equal to $\left|\big(\Phi_1(u)\big)(t_1) - \big(\Phi_1(u)\big)(t_0)\right|$. The remainder of the proof will be carried out by induction, where we assume that

$$|\Phi_1(u)|_{[t_0,t_k]} - c_1 = \mathcal{D}_{[t_0,t_k]}\big(\Phi_2(u)\big) \tag{A.6}$$

is true, and we need to show that

$$|\Phi_1(u)|_{[t_0,t_{k+1}]} - c_1 = \mathcal{D}_{[t_0,t_{k+1}]}\big(\Phi_2(u)\big) \tag{A.7}$$

holds. Using the definition of variation for the interval $[t_0, t_k]$ in Eq. (A.6) gives,

$$\left(\sum_{i=0}^{k-1} \left|\big(\Phi_1(u)\big)(t_{i+1}) - \big(\Phi_1(u)\big)(t_i)\right|\right) = \mathcal{D}_{[t_0,t_k]}\big(\Phi_2(u)\big), \tag{A.8}$$

and similarly for the interval $[t_0, t_{k+1}]$, Eq. (A.7) becomes

$$\left(\sum_{i=0}^{k} \left|\big(\Phi_1(u)\big)(t_{i+1}) - \big(\Phi_1(u)\big)(t_i)\right|\right) = \mathcal{D}_{[t_0,t_{k+1}]}\big(\Phi_2(u)\big). \tag{A.9}$$

Using our assumption in Eq. (A.6), then Eq. (A.9) becomes

$$\mathcal{D}_{[t_0,t_k]}\big(\Phi_2(u)\big) + \left|\big(\Phi_1(u)\big)(t_{k+1}) - \big(\Phi_1(u)\big)(t_k)\right| = \mathcal{D}_{[t_0,t_{k+1}]}\big(\Phi_2(u)\big). \tag{A.10}$$

Following the same step as done for computing Eq. (A.1), it is immediate to calculate that $\left|\big(\Phi_1(u)\big)(t_{k+1}) - \big(\Phi_1(u)\big)(t_k)\right| = \mathcal{D}_{[t_k,t_{k+1}]}\big(\Phi_2(u)\big)$ such that Eq. (A.10) yields

$$\mathcal{D}_{[t_0,t_k]}\big(\Phi_2(u)\big) + \mathcal{D}_{[t_k,t_{k+1}]}\big(\Phi_2(u)\big) = \mathcal{D}_{[t_0,t_{k+1}]}\big(\Phi_2(u)\big), \tag{A.11}$$

which completes the proof if we let $t_0 = 0$ and $t_{k+1} = \eta$. □

References

[1] F. Bagagiolo, Viscosity solutions for an optimal control problem with Preisach hysteresis nonlinearities, ESAIM: Control Optim. Calcul. Var. 10 (02) (2004) 271–294.
[2] J. Barradas-Berglind, R. Wisniewski, Control of linear systems with preisach hysteresis output with application to damage reduction, in: Proceedings of the 2015 European Control Conference (ECC), IEEE, 2015, pp. 3572–3578.
[3] J. Barradas-Berglind, R. Wisniewski, Representation of fatigue for wind turbine control, Wind Energy (2016), doi:10.1002/we.1975.
[4] J. Barradas-Berglind, R. Wisniewski, M. Soltani, Fatigue load modeling and control for wind turbines based on hysteresis operators, in: Proceedings of the American Control Conference (ACC), IEEE, 2015, pp. 3721–3727.
[5] F.D. Bianchi, H. De Battista, R.J. Mantz, Wind Turbine Control Systems: Principles, Modelling and Gain Scheduling Design, Springer Science & Business Media, 2006.
[6] E. Bossanyi, The design of closed loop controllers for wind turbines, Wind Energy 3 (3) (2000) 149–163.
[7] P. van Bree, C. van Lierop, P. van den Bosch, Control-oriented hysteresis models for magnetic electron lenses, IEEE Trans. Magn. 45 (11) (2009) 5235–5238.
[8] M. Brokate, J. Sprekels, Hysteresis and Phase Transitions, volume 121 of Applied Mathematical Sciences, Springer-Verlag, 1996.
[9] E.F. Camacho, C. Bordons, Model Predictive Control, 2, Springer, 2004.
[10] B.D. Coleman, M.L. Hodgdon, On a class of constitutive relations for ferromagnetic hysteresis, Arch. Ration. Mech. Anal. 99 (4) (1987) 375–396.
[11] P.R. Dahl, Solid friction damping of mechanical vibrations, AIAA J. 14 (12) (1976) 1675–1682.
[12] C.C. De Wit, H. Olsson, K.J. Astrom, P. Lischinsky, A new model for control of systems with friction, Autom. Control, IEEE Transactions on 40 (3) (1995) 419–425.
[13] S. Downing, D. Socie, Simple rainflow counting algorithms, Int. J. Fatigue 4 (1) (1982) 31–40.
[14] G. Franklin, J. Powell, A. Emami-Naeini, Feedback Control of Dynamic Systems, 3, Addison-Wesley Reading, 1994.
[15] R.B. Gorbet, Control of hysteretic systems with Preisach representations, (Ph.D. thesis) University of Waterloo, 1998.
[16] R.B. Gorbet, K.A. Morris, D.W. Wang, Passivity-based stability and control of hysteresis in smart actuators, Control Syst. Technol. IEEE Trans. 9 (1) (2001) 5–16.
[17] J.M. Grosso, C. Ocampo-Martínez, V. Puig, A service reliability model predictive control with dynamic safety stocks and actuators health monitoring for drinking water networks, in: Proceedings of the 2012 IEEE Fifty-first IEEE Conference on Decision and Control (CDC), IEEE, 2012, pp. 4568–4573.
[18] F. Ikhouane, J. Rodellar, A linear controller for hysteretic systems, Autom. Control IEEE Trans. 51 (2) (2006) 340–344.
[19] B. Jayawardhana, R. Ouyang, V. Andrieu, Stability of systems with the Duhem hysteresis operator: The dissipativity approach, Automatica 48 (10) (2012) 2657–2662.
[20] D. Jiles, D. Atherton, Theory of ferromagnetic hysteresis, J. Magn. Magn. Mater. 61 (1) (1986) 48–60.
[21] J.M. Jonkman, S. Butterfield, W. Musial, G. Scott, Definition of a 5-MW Reference Wind Turbine for Offshore System Development, NREL, 2009.
[22] U. Krupp, Fatigue Crack Propagation in Metals and Alloys: Microstructural Aspects and Modelling Concepts, John Wiley & Sons, 2007.
[23] J. Löfberg, YALMIP: A toolbox for modeling and optimization in MATLAB, in: Proceedings of the CACSD Conference, Taipei, Taiwan, 2004.
[24] H. Logemann, E.P. Ryan, Systems with hysteresis in the feedback loop: existence, regularity and asymptotic behaviour of solutions, ESAIM: Control Optim. Calcul. Var. 9 (2003) 169–196.
[25] J.M. Maciejowski, M. Huzmezan, Predictive Control with Constraints, Springer, 1997.
[26] J.W. Macki, P. Nistri, P. Zecca, Mathematical models for hysteresis, SIAM Rev. 35 (1) (1993) 94–123.
[27] I.D. Mayergoyz, Mathematical Models of Hysteresis, Springer-Verlag, 1991.

[28] A. Niesłony, Determination of fragments of multiaxial service loading strongly influencing the fatigue of machine components, Mech. Syst. Signal Process. 23 (8) (2009) 2712–2721.
[29] R. Ouyang, Stability analysis and controller design for a system with hysteresis, University of Groningen, 2013 Ph.D. thesis.
[30] R. Ouyang, V. Andrieu, B. Jayawardhana, On the characterization of the Duhem hysteresis operator with clockwise input–output dynamics, Syst. Control Lett. 62 (3) (2013) 286–293.
[31] R. Ouyang, B. Jayawardhana, Absolute stability analysis of linear systems with duhem hysteresis operator, Automatica 50 (7) (2014) 1860–1866.
[32] A. Padthe, J. Oh, D.S. Bernstein, Counterclockwise dynamics of a rate-independent semilinear Duhem model, in: Proceedings of the Forty-forth IEEE Decision and Control and European Control Conference (CDC-ECC), IEEE, 2005, pp. 8000–8005.
[33] F.K. Pour, V. Puig, C. Ocampo-Martinez, Health-aware model predictive control of pasteurization plant, in: J. Phys.: Conf. Ser., 783, IOP Publishing, 2017, p. 012030.
[34] D. Radaj, M. Vormwald, Ermüdungsfestigkeit, Grundl. Leichtbau, Masch. Stahlbau (1995).
[35] I. Rychlik, A new definition of the rainflow cycle counting method, Int. J. Fatigue 9 (2) (1987) 119–121.
[36] D. Schlipf, D.J. Schlipf, M. Kühn, Nonlinear model predictive control of wind turbines using LIDAR, Wind Energy 16 (7) (2013) 1107–1129.
[37] W. Schütz, A history of fatigue, Eng. Fract. Mech. 54 (2) (1996) 263–300.
[38] M. Soltani, R. Wisniewski, P. Brath, S. Boyd, Load reduction of wind turbines using receding horizon control, in: Proceedings of the IEEE International Conference on Control Applications (CCA), 2011, pp. 852–857.
[39] M.N. Soltani, T. Knudsen, M. Svenstrup, R. Wisniewski, P. Brath, R. Ortega, K. Johnson, Estimation of rotor effective wind speed: A comparison, IEEE Trans. Control Syst. Technol. 21 (4) (2013) 1155–1167.
[40] A. Standard, E1049-85, Stand. Pract. Cycle Count. Fatigue Anal. ASTM (2011).
[41] A. Visintin, Differential Models of Hysteresis, Springer Berlin, 1994.
[42] J.C. Willems, Dissipative dynamical systems part I: General theory, Arch. Ration. Mech. Anal. 45 (5) (1972) 321–351.